



AFRL-AFOSR-VA-TR-2022-0066

Tunable Porous and Patterned Surfaces for Turbulence Control

Luhar, Mitul
UNIVERSITY OF SOUTHERN CALIFORNIA
3720 S FLOWER ST FL 3
LOS ANGELES, CA, 90007
USA

12/15/2021
Final Technical Report

DISTRIBUTION A: Distribution approved for public release.

Air Force Research Laboratory
Air Force Office of Scientific Research
Arlington, Virginia 22203
Air Force Materiel Command

REPORT DOCUMENTATION PAGE

Form Approved
OMB No. 0704-0188

The public reporting burden for this collection of information is estimated to average 1 hour per response, including the time for reviewing instructions, searching existing data sources, gathering and maintaining the data needed, and completing and reviewing the collection of information. Send comments regarding this burden estimate or any other aspect of this collection of information, including suggestions for reducing the burden, to Department of Defense, Washington Headquarters Services, Directorate for Information Operations and Reports (0704-0188), 1215 Jefferson Davis Highway, Suite 1204, Arlington, VA 22202-4302. Respondents should be aware that notwithstanding any other provision of law, no person shall be subject to any penalty for failing to comply with a collection of information if it does not display a currently valid OMB control number.
PLEASE DO NOT RETURN YOUR FORM TO THE ABOVE ADDRESS.

1. REPORT DATE (DD-MM-YYYY) 15-12-2021	2. REPORT TYPE Final	3. DATES COVERED (From - To) 01 Feb 2017 - 15 Aug 2021
--	--------------------------------	--

4. TITLE AND SUBTITLE Tunable Porous and Patterned Surfaces for Turbulence Control	5a. CONTRACT NUMBER
	5b. GRANT NUMBER FA9550-17-1-0142
	5c. PROGRAM ELEMENT NUMBER 61102F

6. AUTHOR(S) Mitul Luhar	5d. PROJECT NUMBER
	5e. TASK NUMBER
	5f. WORK UNIT NUMBER

7. PERFORMING ORGANIZATION NAME(S) AND ADDRESS(ES) UNIVERSITY OF SOUTHERN CALIFORNIA 3720 S FLOWER ST FL 3 LOS ANGELES, CA 90007 USA	8. PERFORMING ORGANIZATION REPORT NUMBER
---	---

9. SPONSORING/MONITORING AGENCY NAME(S) AND ADDRESS(ES) AF Office of Scientific Research 875 N. Randolph St. Room 3112 Arlington, VA 22203	10. SPONSOR/MONITOR'S ACRONYM(S) AFRL/AFOSR RTA1
	11. SPONSOR/MONITOR'S REPORT NUMBER(S) AFRL-AFOSR-VA-TR-2022-0066

12. DISTRIBUTION/AVAILABILITY STATEMENT
A Distribution Unlimited: PB Public Release

13. SUPPLEMENTARY NOTES

14. ABSTRACT
Research supported by this grant targeted the development of passive control techniques for wall-bounded turbulent flows. Advances in additive manufacturing technology have opened a vast new design space in the development of multi-functional surfaces and materials that can passively control turbulent flows. However, the design and optimization of substrate microstructure to yield a desired response in the overlying turbulent flow remains a challenge. To address this challenge, reduced-complexity models were developed to predict how specific surface treatments modify the near-wall flow field with minimal computation. These models were grounded in the resolvent formalism, which leverages a gain-based decomposition to identify key features of the turbulent flow field. Model predictions showed that the drag reduction performance of so-called riblet surfaces (which have successfully demonstrated drag reduction in prior laboratory experiments and flight tests) correlates well with the amplification or suppression of a single near-wall flow structure. The development of this efficient surrogate model enabled optimization of 2D riblet geometry, preliminary consideration of 3D riblets, as well as the model-guided development of anisotropic porous materials for passive friction reduction in turbulent flows. Model predictions were used to guide the design and fabrication (via 3D printing) of anisotropic porous materials for preliminary laboratory experiments.

15. SUBJECT TERMS

16. SECURITY CLASSIFICATION OF:			17. LIMITATION OF ABSTRACT	18. NUMBER OF PAGES	19a. NAME OF RESPONSIBLE PERSON GREGG ABATE
a. REPORT	b. ABSTRACT	c. THIS PAGE			19b. TELEPHONE NUMBER (Include area code)
U	U	U	UU	19	425-1779

Standard Form 298 (Rev.8/98)
Prescribed by ANSI Std. Z39.18

Tunable Porous and Patterned Surfaces for Turbulence Control (YIP)

Principal Investigator:

Mitul Luhar

Associate Professor

Department of Aerospace and Mechanical Engineering
University of Southern California, Los Angeles, CA 90089

luhar@usc.edu

Award Number:

FA9550-17-1-0142

Program Manager(s):

Dr. Douglas Smith, Dr. Gregg Abate

Final Report

Contents

Abstract.....	3
1. Accomplishments.....	4
1.1 Overview	4
1.2 Specific Objectives	4
1.3 Dissemination of Results.....	5
1.3.1 Archival Journal publications	5
1.3.2 Peer-reviewed conference publications	6
1.3.3 Contributed Talks	6
1.3.4 In preparation or submitted	7
2. Technical Developments.....	7
2.1 Reduced-Complexity Models.....	7
2.1.1 2D Riblets	8
2.1.2 Riblet Geometry Optimization	9
2.1.3 3D Riblets	10
2.1.4 Anisotropic Porous Materials.....	10
2.1.5 Model Limitations and Outlook	11
2.2 Laboratory Experiments.....	12
2.2.1 Commercially Available Foams	12
2.2.2 3D-printed Anisotropic Materials	13
2.2.3 Outlook	15
3. Impact	16
3.1 Impact on Disciplinary Field	16
3.2 Development of Human Resources	17
References	18

Abstract

Approved for Public Release

Research supported by this grant targeted the development of passive control techniques for wall-bounded turbulent flows. Advances in additive manufacturing technology have opened a vast new design space in the development of multi-functional surfaces and materials that can passively control turbulent flows. However, the design and optimization of substrate microstructure to yield a desired response in the overlying turbulent flow remains a challenge. To address this challenge, reduced-complexity models were developed to predict how specific surface treatments modify the near-wall flow field with minimal computation. These models were grounded in the resolvent formalism, which leverages a gain-based decomposition to identify key features of the turbulent flow field. Model predictions showed that the drag reduction performance of so-called riblet surfaces (which have successfully demonstrated drag reduction in prior laboratory experiments and flight tests) correlates well with the amplification or suppression of a single near-wall flow structure. The development of this efficient surrogate model enabled optimization of 2D riblet geometry, preliminary consideration of 3D riblets, as well as the model-guided development of anisotropic porous materials for passive friction reduction in turbulent flows. Model predictions were used to guide the design and fabrication (via 3D printing) of anisotropic porous materials for preliminary laboratory experiments.

1. Accomplishments

1.1 Overview

Research supported by this grant targeted the development of control techniques for wall-bounded turbulent flows (e.g., boundary layers, channel and duct flows, pipe flows). This effort emphasized *passive* control techniques that do not require real-time sensing and actuation or complex feedback control. In particular, the project focused on the development of surfaces and materials that can reduce turbulent skin friction drag. Examples includes surfaces with streamwise-aligned *riblets* (see e.g., Bechert et al., 1997) that have shown as much as 10% drag reduction in previous laboratory experiments (up to 2% drag reduction in flight tests) as well as anisotropic permeable materials, which have shown up to 25% drag reduction in highly idealized numerical simulations (Gomez-De-Segura & Garcia-Mayoral, 2019).

Advances in additive manufacturing have enabled the fabrication of substrates with near-arbitrary microstructure for certain classes of materials. Spatial resolution and material-handling capabilities continue to improve. This has opened a vast new design space in the development of multi-functional surfaces that can passively control turbulent flows. However, the design and optimization of surface microstructure to yield a desired response in the overlying turbulent flow (i.e., modifying the integrated momentum balance or turbulence spectrum) remains a challenge.

Research carried out under this grant has led to the development of reduced-complexity models that can predict how specific surface treatments modify the near-wall flow field with minimal computation. Model predictions showed that the drag reduction performance of riblets and anisotropic porous materials (Bechert et al., 1997; Garcia-Mayoral & Jimenez, 2011; Gomez-de-Segura et al., 2018; Rosti et al., 2018) correlates well with the amplification or suppression of a single near-wall flow structure, or mode, identified via a gain-based decomposition of the governing Navier-Stokes equations (Chavarin & Luhar, 2020). The development of this computationally efficient surrogate model has enabled optimization of riblet geometry as well as model-based design of porous materials for passive friction reduction in turbulent flows. Model predictions were also used to design and fabricate anisotropic porous materials for proof-of-concept laboratory experiments.

The remainder of this report is structured as follows. Specific objectives for the project are listed in Section 1.2. Section 1.3 provides a listing of the results generated under this grant. Specific technical accomplishments are discussed in Section 2. Section 2.1 focuses on the modeling and optimization effort while Section 2.2 focuses on experiments. Section 3 discusses the impact of the grant on the disciplinary field (Section 3.1) and the development of human resources (Section 3.2), and the external collaborations enabled by this research.

1.2 Specific Objectives

The specific objectives of this research, as identified in the original proposal, were as follows:

- Objective 1: Develop a unified modeling framework that generates rapid predictions for how a specific surface treatment modifies the turbulent flow field.

- Objective 2: Verify model predictions for turbulent spectra and conditionally-averaged flow structure via laboratory experiments.
- Objective 3: Leverage the modeling framework to design surface treatments that can predictably alter the turbulent flow for a given control objective.

These objectives combine model development, optimization, as well as laboratory testing. These components are discussed further in Section 2.

1.3 Dissemination of Results

Results generated from this effort were disseminated via the following publications and presentations.

1.3.1 Archival Journal publications

- Chavarin, A., Gomez-de-Segura, G., Garcia-Mayoral, R., & Luhar, M. (2021). Resolvent-based predictions for turbulent flow over anisotropic permeable substrates. *Journal of Fluid Mechanics*, 913, A24.

<https://doi.org/10.1017/jfm.2020.1169>

- Chavarin, A., Efstathiou, C., Vijay, S., & Luhar, M. (2020). Resolvent-based design and experimental testing of porous materials for passive turbulence control. *International Journal of Heat and Fluid Flow*, 86, 108722.

<https://doi.org/10.1016/j.ijheatfluidflow.2020.108722>

- Chavarin, A., & Luhar, M. (2020). Resolvent analysis for turbulent channel flow with riblets. *AIAA Journal*, 58(2), 589-599.

<https://doi.org/10.2514/1.J058205>

- Kawagoe, A., Nakashima, S., Luhar, M., & Fukagata, K. (2019). Proposal of control laws for turbulent skin friction reduction based on resolvent analysis. *Journal of Fluid Mechanics*, 866, 810-840.

<https://doi.org/10.1017/jfm.2019.157>

- Efstathiou, C., & Luhar, M. (2018). Mean turbulence statistics in boundary layers over high-porosity foams. *Journal of Fluid Mechanics*, 841, 351-379.

<https://doi.org/10.1017/jfm.2018.57>

- Nakashima, S., Fukagata, K., & Luhar, M. (2017). Assessment of suboptimal control for turbulent skin friction reduction via resolvent analysis. *Journal of Fluid Mechanics*, 828, 496-526.

<https://doi.org/10.1017/jfm.2017.519>

1.3.2 Peer-reviewed conference publications

- Chavarin, A., Vijay, S., Efstathiou, C., & Luhar, M. (2019) Resolvent-based design and experimental testing of porous materials for passive turbulence control, *11th International Symposium on Turbulence and Shear Flow Phenomena (TSFP11)*, Southampton, UK.
- Efstathiou, C., & Luhar, M. (2017) Turbulent boundary layer measurements over permeable surfaces, *10th International Symposium on Turbulence and Shear Flow Phenomena (TSFP10)*, Chicago, USA
- Luhar, M. (2017) Low-order models for turbulent flows over complex walls, *10th International Symposium on Turbulence and Shear Flow Phenomena (TSFP10)*, Chicago, USA

1.3.3 Contributed Talks

- Chavarin, A., & Luhar, M. (2020) Model-based Predictions for Optimal 2D Riblet Geometries, *AIAA SciTech, Invited AIAA-JSASS joint session on Boundary Layer Modification*.
- Luhar, M., & Chavarin, A. (2019). A minimal model for riblet geometry optimization. *Bulletin of the American Physical Society*.
- Efstathiou, C., & Luhar, M. (2019). Measurements in turbulent boundary layers over designed anisotropic porous materials. *Bulletin of the American Physical Society*.
- Chavarin, A., Gomez-de-Segura, G., Garcia-Mayoral, R., & Luhar, M. (2019). Resolvent-informed design of anisotropic permeable substrates for turbulence control. *Bulletin of the American Physical Society*.
- Chavarin, A., & Luhar, M. (2019). Optimization of Riblet Geometry using Low-order Models. *AIAA Aviation, Invited Session on Reduced-Complexity Modeling and Flow Control*
- Efstathiou, C., Todt, A., & Luhar, M. (2018). A novel method to measure 3D permeability of highly porous materials. *Bulletin of the American Physical Society*.
- Chavarin, A., & Luhar, M. (2018). Optimization of two dimensional riblet geometries using the Resolvent analysis. *Bulletin of the American Physical Society*.
- Chavarin, A., & Luhar, M. (2018). Resolvent Analysis for Turbulent Flow over Patterned Walls. *AIAA Aviation, Invited Session on Modal Analysis Methods*.
- Efstathiou, C., & Luhar, M. (2017). Turbulent boundary layer measurements over permeable substrates. *Bulletin of the American Physical Society*.

1.3.4 In preparation or submitted

- Chavarin, A., & Luhar, M. (2022) Optimization of Riblet Geometry via the Resolvent Framework, *AIAA SciTech*
- Efstathiou, C., & Luhar, M. (2021) Turbulent boundary layer measurements over streamwise-preferential porous materials, *in revision*

2. Technical Developments

2.1 Reduced-Complexity Models

This award enabled an extension of the resolvent formalism for wall-bounded turbulent flows (McKeon & Sharma, 2010) to account for more complex surfaces. Briefly, the resolvent formulation identifies highly-amplified propagating structures via a gain-based decomposition of the governing equations. A central advantage of this theoretical framework is that it can account for nonlinear energy transfer, while emphasizing the linear dynamics that are known to be important in turbulent shear flows. For wall-bounded flows that are approximately homogeneous in the streamwise and spanwise directions and stationary in time, the momentum equations and continuity constraint can be Fourier-transformed and expressed compactly as

$$\begin{bmatrix} \mathbf{u}_{\mathbf{k}} \\ p_{\mathbf{k}} \end{bmatrix} = (-i\omega - \mathbf{L}_{\mathbf{k}})^{-1} = \mathbf{H}_{\mathbf{k}} \mathbf{f}_{\mathbf{k}}.$$

Here, $\mathbf{u}_{\mathbf{k}}(y)$ and $p_{\mathbf{k}}(y)$ are the complex Fourier coefficients for a given wavenumber-frequency combination $\mathbf{k} = (\kappa_x, \kappa_z, \omega)$, $\mathbf{f}_{\mathbf{k}} = (\mathbf{u} \cdot \nabla \mathbf{u})_{\mathbf{k}}$ denotes the nonlinear term, $\mathbf{L}_{\mathbf{k}}$ is the linear Navier-Stokes operator, and $\mathbf{H}_{\mathbf{k}}$ is the resolvent. A singular value decomposition (SVD) of an appropriately weighted and discretized resolvent operator, $\hat{\mathbf{H}}_{\mathbf{k}} = \Psi \Sigma \Phi$, identifies flow structures that are highly amplified across spectral space.

Specific high gain response modes (i.e., the rank-1 left singular vector, ψ_1) serve as useful surrogates for dynamically important flow features such as the self-sustaining near-wall (NW) cycle as well as larger-scale structures found further from the wall (Smits et al., 2011). Therefore, as a starting point, the effect of any active or passive control technique can be evaluated just on these individual ‘resolvent modes’ – at greatly reduced computational cost compared to higher-fidelity numerical simulations (see e.g., Luhar et al., 2014; Nakashima et al., 2017).

The effect of more complex surfaces is included in the resolvent framework via modification to the governing equations and boundary conditions (Chavarin & Luhar, 2020; Chavarin et al., 2021). Predictions made using this extended modeling framework have been tested against previous high-fidelity simulation results for flow over streamwise constant riblets (Garcia-Mayoral & Jimenez, 2011) as well as anisotropic permeable materials (Gomez-de-Segura and Garcia-Mayoral, 2019). Key results for riblets and porous materials are presented below.

2.1.1 2D Riblets

The use of streamwise-aligned riblets is arguably one of the simplest and most effective passive turbulence control techniques tested thus far. Previous experiments and simulations have shown drag reductions as large as 10% for specific riblet geometries (e.g., Bechert et al., 1997; Garcia-Mayoral & Jimenez, 2011). Riblets have also been tested with limited success in flight tests.

Previous research on riblets has provided significant physical insight into riblet performance. It is generally accepted that the drag-reducing ability of such surfaces arises from their anisotropy: riblets offer much less resistance to streamwise flows compared to spanwise flows. Thus, the mean flow in the streamwise direction is essentially unimpeded within the riblet grooves, generating high interfacial slip. However, the counter-rotating vortices associated with the near-wall turbulence are pushed up above the riblet tips and suppressed. This decreases the turbulent transfer of momentum in the wall-normal direction, reducing drag. Drag reduction initially increases linearly with riblet size, but beyond a certain threshold, the NW vortices either lodge into the grooves or interact with the riblet tips to create secondary vorticity. This leads to greater turbulence penetration into the grooves and increases skin friction. Specific riblet geometries are also susceptible to a Kelvin-Helmholtz type instability.

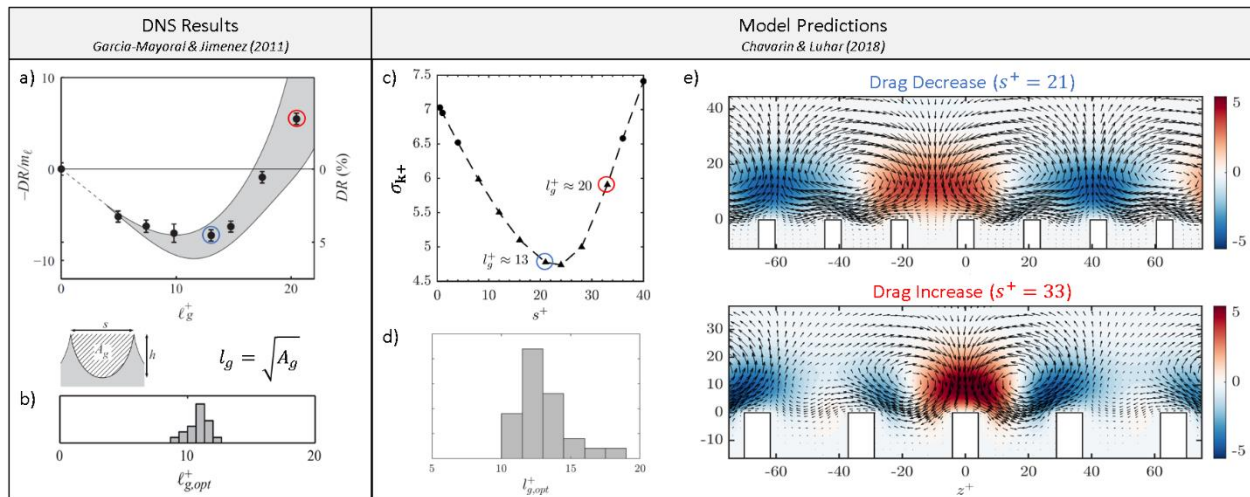


Figure 1. A comparison of DNS results (a,b) and model-based predictions (c-e) for 2D riblets. (a) Drag reduction obtained in DNS over rectangular riblets of varying size. (b) Distribution of optimal riblet sizes based on compilation of prior simulation and experiments (Bechert et al., 1997; Garcia-Mayoral & Jimenez, 2011). (c) Model predictions for gain for a single mode over rectangular riblets of varying size. (d) Predicted distribution of optimal sizes for a variety of 2D riblet geometries. (e) Predicted change in structure of resolvent mode over drag-reducing (top) and drag-increasing (bottom) rectangular riblets.

The extended resolvent framework developed here (Chavarin & Luhar, 2020) embeds the effect of the riblets into the governing equations via volume penalization prior to pursuing the gain-based decomposition. This approach reproduces all the physical effects discussed above. For instance, this effort has demonstrated that the gain for the NW resolvent mode (Figure 1c) is a useful surrogate for the total drag reduction obtained in high-fidelity direct numerical simulations (DNS, Figure 1a) over rectangular riblets of varying size. Moreover, the distribution of optimal

riblet geometries, identified based on gain minima for a variety of rectangular, triangular, and trapezoidal 2D riblet geometries (Figure 1d), is remarkably close to the distribution obtained in previous experiments and simulations (Figure 1b). Predicted changes in NW mode structure (Figure 1e) for the drag-reducing and drag-increasing cases are also consistent with prior observations.

2.1.2 Riblet Geometry Optimization

Each resolvent mode evaluation for 2D riblets takes less than 60s on one core of a workstation, and Reynolds number penalties are not significant. Therefore, the results presented in Figure 1 indicate that the extended resolvent framework can serve as a powerful optimization tool prior to testing in high-fidelity simulations and laboratory experiments. Building on this insight, we have developed an optimization framework for the geometry of 2D riblets. This optimization framework parametrizes riblet shape using Bezier curves. Salient points for the Bezier curves, which determine riblet spacing, height, and cross-sectional shape are then determined via a gradient-based search. The parameter combination that minimizes the gain for the NW resolvent mode is identified as the optimal geometry.

An important advantage of this approach is that it enables geometry optimization under any manufacturing constraints (e.g., minimum thickness, radius of curvature, etc.). As an example, the images in Figure 2 show the optimal geometries identified for riblets with varying minimum radius of curvature at the tips. Moreover, the framework can generate predictions for the high Reynolds numbers expected in real-world applications.

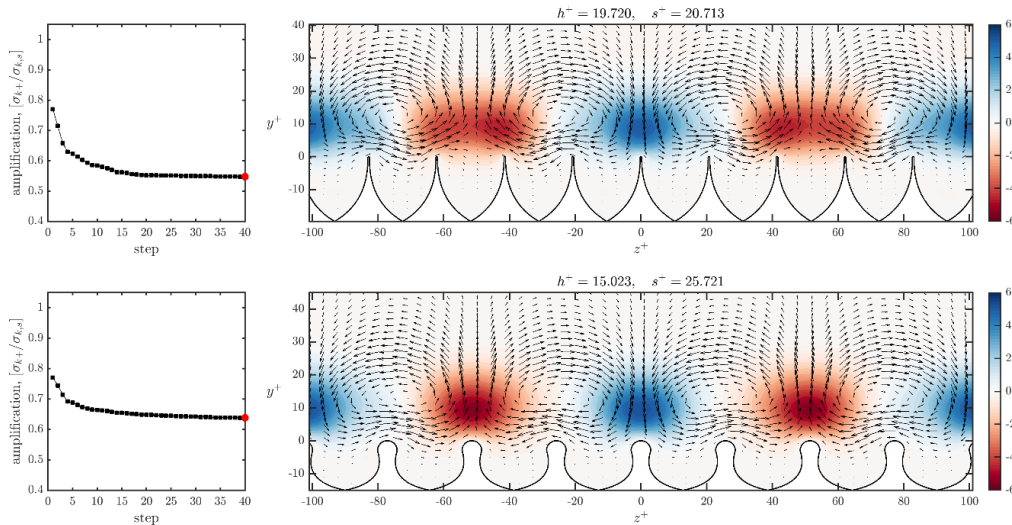


Figure 2. Images showing optimal geometries identified at the termination of the gradient-based search for 2D riblets with varying radius of curvature at the tips: $r_c^+ = 0.25$ (top) and $r_c^+ = 3.0$ (bottom). Values of h^+ and s^+ denote the height and the center-center spacing for the riblets. A superscript + denotes normalization with respect to friction velocity and viscosity.

2.1.3 3D Riblets

We have also pursued extension of the modeling framework to three-dimensional (3D) riblets, which have the potential to outperform 2D riblets (McClure et al. 2020). The extension to 3D riblets introduces additional complexity and computational cost since the flow can no longer be considered homogeneous in the streamwise direction. The modeling effort for 2D riblets assumed that the base flow and geometry were homogeneous in the streamwise direction, which allowed for consideration of streamwise Fourier modes in the resolvent analysis framework. For 3D riblets, the coupling between these Fourier modes and the streamwise variation in riblet geometry (and base flow) needs to be considered.

Preliminary results for 3D riblets (presented at the 2021 AFOSR program review meeting; not shown here) suggest that additional decreases in NW mode gain are possible for appropriately chosen gaps in riblet geometry in the streamwise direction. This is indicative of greater drag reduction compared to 2D riblets. However, additional work is needed to verify these predictions and characterize the underlying flow physics. Since there are few previous experimental or high-fidelity computations exploring the effects of 3D riblet geometry, a key bottleneck is the lack of data for model validation.

2.1.4 Anisotropic Porous Materials

Previous simulation results suggest that materials with high streamwise permeability (K_x) and low wall-normal (K_y) and spanwise (K_z) permeabilities can generate substantial skin friction reductions of up to 25% (Gomez-de-Segura et al., 2018; Rosti et al., 2018; Gomez-de-Segura & Garcia-Mayoral 2019). The physical mechanism responsible for drag reduction over anisotropic porous materials is similar to the mechanism responsible for drag reduction with riblets. High porosity and streamwise permeability contribute to a substantial interfacial slip velocity, while low wall-normal and spanwise permeability limit turbulence penetration into the porous substrate. A Kelvin-Helmholtz-type instability is also expected to arise over porous materials with high wall-normal permeability. The extended resolvent framework is again able to reproduce these prior observations. In this case, the effect of the permeable material is included in the resolvent framework using the well-known Darcy-Forchheimer formulation (i.e., via appropriate permeability and Forchheimer coefficients; see e.g., Breugem et al., 2006).

The predictive power of the modeling framework is showcased by the sample results shown in Figure 3 and Figure 4 for flow over anisotropic porous materials (Chavarin et al., 2021). Figure 3a shows that the forcing-response gain for the NW resolvent modes is a very good predictor of the friction reduction observed in numerical simulations (Gomez-de-Segura & Garcia-Mayoral, 2019). Material properties that lead to a suppression in gain relative to the smooth wall case (red curve) yield an outward shift in the mean velocity profile (black curve) and, hence, drag reduction in simulations. Further, the initial decrease in singular values is linearly proportional to difference between the square root of the streamwise and spanwise permeabilities, $\sqrt{K_x} - \sqrt{K_z}$ across all cases, which is consistent with our qualitative understanding of such flows.

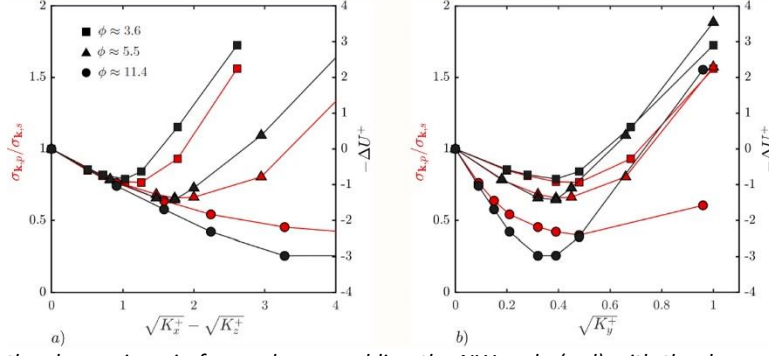


Figure 3 Comparison of the change in gain for modes resembling the NW cycle (red) with the drag reduction observed in DNS (black; from Gomez-de-Segura et al., 2018) over anisotropic porous materials. Symbols denote substrates with different anisotropy ratios, $\phi = \sqrt{K_x}/\sqrt{K_y}$.

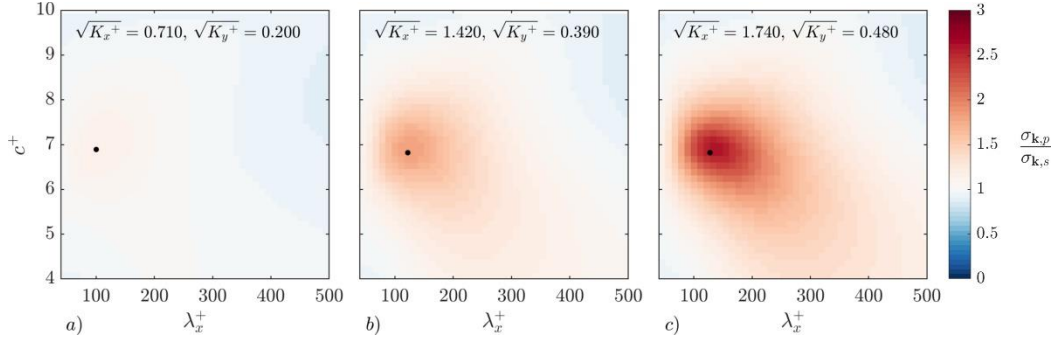


Figure 4 Change in singular values for spanwise-constant resolvent modes of varying streamwise wavelength (λ_x^+) and mode speed (c^+). Wall-normal permeability increases from (a)-(c) but the anisotropy ratio is fixed, $\phi = \sqrt{K_x}/\sqrt{K_y} \approx 3.6$.

Figure 3b shows that the gain for the NW resolvent mode alone does not predict the exact conditions in which performance deteriorates. Simulation data show that performance deteriorates as the wall-normal permeability increases beyond $\sqrt{K_y^+} \approx 0.4$. In the simulations, this coincides with the emergence of spanwise-coherent rollers that resemble Kelvin-Helmholtz vortices and have a streamwise length scale of about 150 viscous units. Figure 4 shows that the resolvent framework predicts the emergence of such structures as well. A region of high amplification is observed for spanwise-constant resolvent modes with $\lambda_x^+ \approx 100 - 150$ for the materials with $\sqrt{K_y^+} \geq 0.39$.

2.1.5 Model Limitations and Outlook

There are some limitations associated with the resolvent-based models discussed above. First, resolvent analysis requires knowledge of the mean profile, which may not be known a priori for turbulent flows over complex substrates. The results presented above made use of mean profiles generated using very simple models (i.e., analytic eddy viscosity profiles) for 2D riblets and anisotropic porous materials. However, for 3D riblets, additional lower-fidelity simulations (in

ANSYS Fluent) were needed. The accuracy of these predictions is questionable, which also makes the resulting model predictions unreliable. Further research evaluating the sensitivity of model predictions to uncertainties in the mean profile would be valuable.

A key strength of the resolvent analysis framework is that it requires modest computational resources. Model predictions can be generated at minimal computational cost for homogeneous substrates (i.e., on a laptop or workstation). Extension to spatially varying substrates does lead to an increase in computational expense due an increase in the size of the linear resolvent operator used for the gain-based decomposition. However, emerging matrix approximation techniques (e.g., randomized algorithms) are likely to alleviate these computational challenges and enable the evaluation of more complex surfaces for flow control in the future.

2.2 Laboratory Experiments

In addition to the modeling effort described above, a concurrent experimental effort aimed to develop and test anisotropic porous materials with permeabilities identified by the resolvent model as being beneficial for drag reduction in wall-bounded turbulent flows. The experimental effort initially focused on characterizing turbulent flows over commercially available high-porosity foams (Section 2.2.1). In addition to providing useful insight into the turbulent flow physics expected over porous materials, these experiments also enabled the development of the boundary layer setup used for subsequent experiments over 3D-printed materials (Section 2.2.2).

2.2.1 Commercially Available Foams

A flat-plate boundary layer setup capable of generating flows with moderate friction Reynolds number (up to $Re_\tau \approx 2000$) and relatively large boundary layer thickness ($\delta > 5\text{cm}$) was developed for the free-surface water channel facility at USC. This set up is shown in Figure 7 below. This flat plate had a cutout towards the trailing edge to accommodate flush-mounted porous materials of varying thickness. The first set of experiments conducted tested the effects of commercially available high porosity polymer foams on boundary layer properties (Efstathiou & Luhar, 2018). Measurements were made below the plate to avoid free-surface effects. A Laser Doppler Velocimeter (LDV) was used to generate point measurements of streamwise and wall-normal velocity.

These measurements confirmed that the turbulent boundary layer is modified substantially over the porous foams relative to smooth-wall conditions. Development data after the smooth-to-porous wall transition suggest that the boundary layer adjusts quickly to the presence of the porous substrate. For most of the foams tested, the mean velocity profile adjusts to a new equilibrium over a streamwise distance $< 10\delta$, which is similar to the adjustment length observed in the transition from smooth to rough walls.

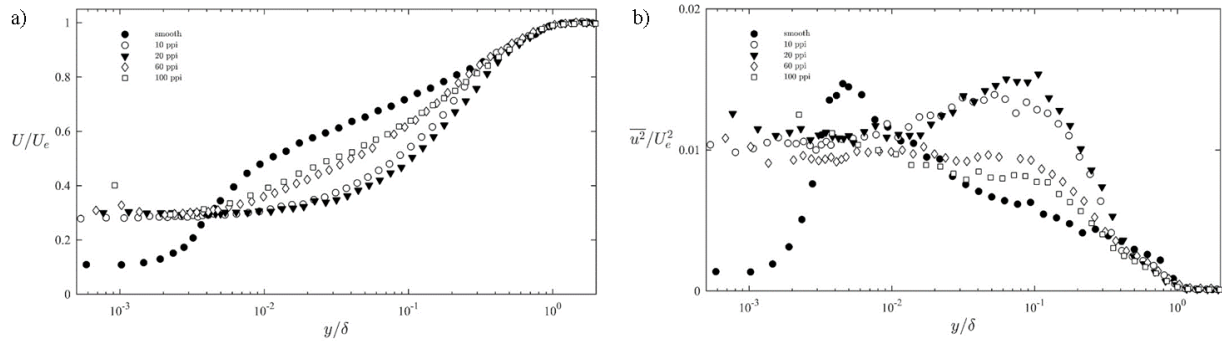


Figure 5 Measured profiles of mean velocity, U/U_e , (a) and streamwise intensity, $\overline{u^2}/U_e^2$, (b) over commercially-available porous foams with systematically-varying pore sizes (from 10 pores per inch to 100 pores per inch).

Fully developed mean velocity profiles (Figure 5a) show the presence of substantial interfacial slip velocities that are relatively insensitive to pore size and porous medium thickness; this observation remains to be explained fully. Profiles of streamwise intensity (Figure 5b) show the emergence of an outer peak at $y/\delta \approx 0.1$ over the porous substrates, which is associated with large-scale structures of length $2\delta - 4\delta$ (wavenumber spectra not shown here for brevity). Such structures have been observed in previous simulations and experiments and are thought to arise from a Kelvin-Helmholtz instability. Skewness data indicate that these large-scale structures can have a modulating effect on the interfacial turbulence. Together, these observations and model predictions from Section 2.1 suggest that suppression of Kelvin-Helmholtz type structures is central to the development of passive substrates that can effectively control turbulence. Further details regarding the porous foam measurements can be found in Efstathiou & Luhar (2018).

2.2.2 3D-printed Anisotropic Materials

After the commercial porous foam tests, experiments focused on the development and testing of anisotropic porous materials for passive flow control. Preliminary results obtained in a benchtop channel flow facility with 3D-printed materials can be found in Chavarin et al. (2020). However, this early set of experiments considered very low Reynolds numbers and the benchtop channel flow facility allowed for limited flow development. More recent experiments have focused on evaluating the effect of streamwise-preferential permeable materials in larger-scale turbulent boundary layer experiments in the free surface water channel facility at friction Reynolds numbers between $Re_\tau \approx 300$ and $Re_\tau \approx 2000$. For these experiments, anisotropic porous materials with a cubic microstructure were designed and fabricated using stereolithographic 3D printing (formlabs Form2). The fabricated materials had a streamwise permeability corresponding to $\sqrt{K_x^+} \approx 2.7$ and wall-normal or spanwise permeabilities $\sqrt{K_y^+} = \sqrt{K_z^+} \approx 0.4$ at the lowest Reynolds number. Sample images showing the 3D-printed porous tiles are provided in Figure 6. This parameter range satisfies the design guidelines from simulations and model predictions, which require that $K_x \geq (K_y, K_z)$ for drag reduction. However, due 3D printing constraints, the magnitude of the wall-normal permeability is above

the threshold ($\sqrt{K_y^+} \approx 0.35$) for the emergence of spanwise-coherent rollers that degrade performance. As a result, no significant drag reduction was expected.

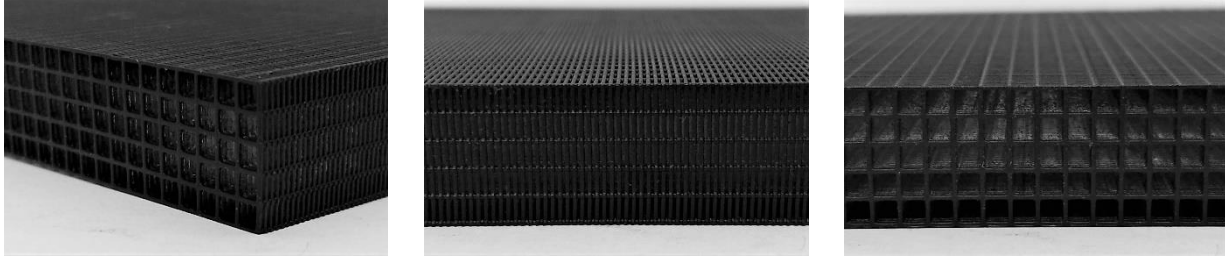


Figure 6 Sample images showing an oblique, side, and front view of the anisotropic porous materials being 3D printed for laboratory experiments. The total thickness of the porous tile is 15.4mm. These tiles were flush-mounted in a flat plate turbulent boundary layer setup. A total of 54 tiles were required for this system.

The 3D-printed porous materials were flush-mounted into the flat plate boundary layer setup shown in Figure 7. A high-speed Particle Image Velocimetry (PIV) system capable of generating measurements at rates up to 2000 Hz was used to generate 2D-2C measurements at one location upstream of the porous substrate and five locations along the substrate. A novel analysis technique was developed to estimate the mean velocity profile at single-pixel resolution in the wall-normal direction (Efstathiou & Luhar, 2020). Mean profiles measured upstream of the porous medium, and at location (5), towards the downstream end of the porous section are shown in Figure 8. As expected, the mean profiles measured upstream of the porous medium are consistent with profiles generated in direct numerical simulations at comparable Reynolds number. However, mean profiles measured over the porous substrate show presence of a slip velocity with magnitude $U_s^+ \approx \sqrt{K_x^+}$, which is consistent with theoretical predictions. The mean profiles also show evidence of outer layer similarity.

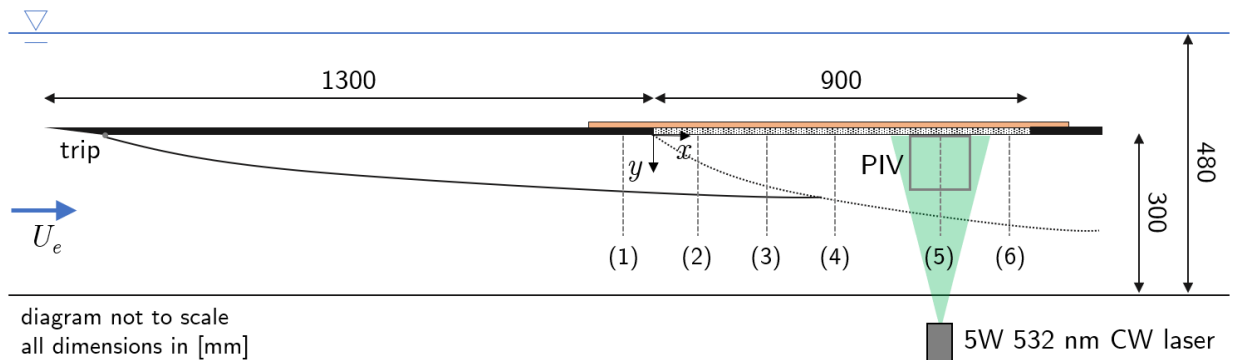


Figure 7 Schematic showing setup for turbulent boundary layer experiments over porous materials. The porous substrate is flush-mounted into a cutout towards the downstream end of the plate. Velocity measurements are made using a high-speed PIV system.

Given the outer layer similarity, fits to the overlap and wake regions of the flow were used to *estimate* boundary layer thickness, friction velocity, and log-layer constants over the smooth wall and porous substrates. These estimates are shown in Figure 9. As expected, the boundary layer thickness grows more slowly over the porous substrate compared to a smooth wall. This is indicative of flow penetration into the porous substrate.

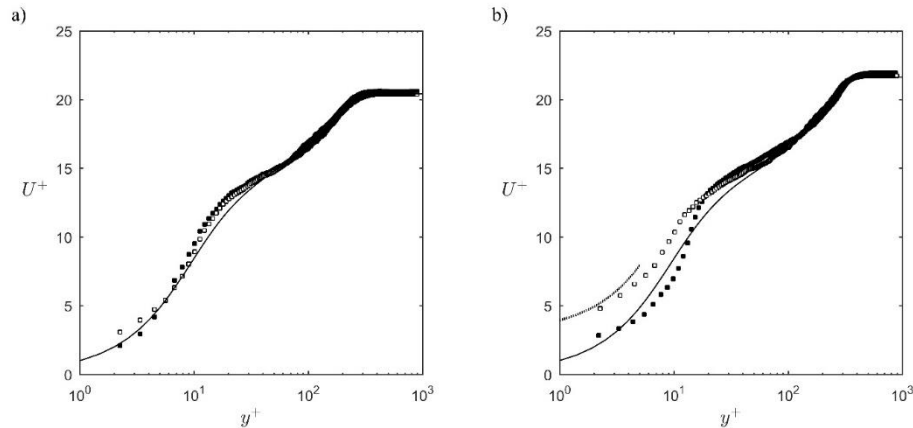


Figure 8 Mean velocity profiles measured upstream of the porous section (a) and at location (5) towards the downstream end of the porous section (b). The filled symbols show measurements over a solid, smooth wall while the open symbols show measurements over the porous material. The solid black line shows mean velocity profiles from Direct Numerical Simulations (DNS) at comparable Reynolds number

After initial development, the friction velocities estimated over the porous substrate are slightly higher (<4%) compared to the corresponding smooth wall values. This difference is comparable to the uncertainty in the friction velocity estimates. Thus, the porous substrates tested do not yield a significant change in friction velocity. This is consistent with resolvent-based predictions and previous numerical simulations, which suggest that material with wall-normal permeability $\sqrt{K_y}^+ \approx 0.4$ can give rise to KH rollers that compromise drag reduction.

2.2.3 Outlook

Drag reduction is predicted to arise over anisotropic porous materials due to the differing slip lengths perceived by the streamwise mean flow and the cross-plane turbulent flow. The idealized simulation results and model predictions discussed above rely on the assumption that these slip lengths can be adequately predicted using bulk properties such as streamwise and spanwise permeability. However, the exact interfacial geometry of the porous material is expected to play an important role in dictating streamwise and transverse slip lengths. These effects need to be explored further. Future work should target the development of materials with bulk properties *and* interfacial geometries that give rise to the desired anisotropy in perceived slip lengths.

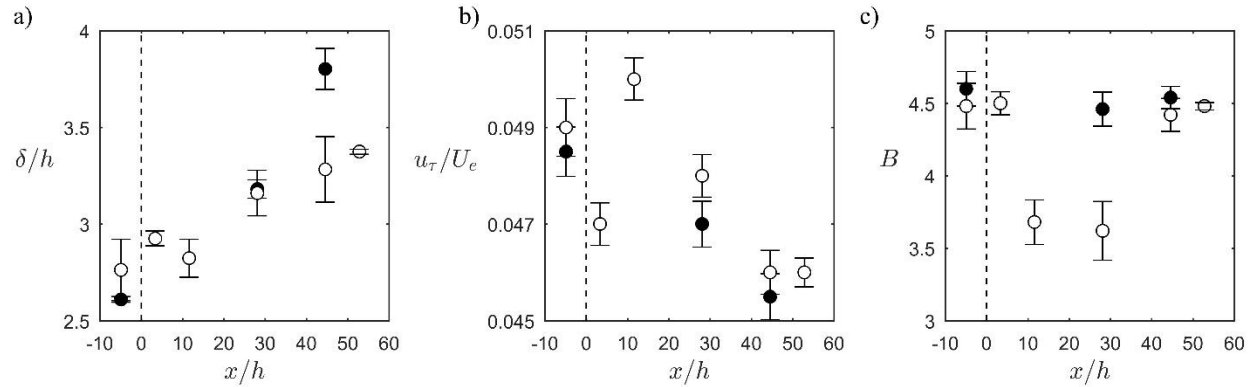


Figure 9 Estimates for boundary layer thickness (a), normalized friction velocity (b), and log-layer constant (c) as a function of streamwise location over the porous section. Open symbols denote measurements over the porous substrate, closed symbols show corresponding measurements over a solid smooth wall.

3. Impact

3.1 Impact on Disciplinary Field

Research supported by this grant led to the development of computationally efficient models that can be used to design porous and patterned surfaces for turbulence control. Specifically, these models were shown to reproduce drag reduction trends observed in previous experiments and high-fidelity simulations for *riblet* surfaces with minimal computation (~ 60 s on a laptop or workstation). This modeling success led to the development of an optimization framework for riblet geometry that can account for manufacturing constraints and be used at applicant-relevant Reynolds numbers.

The modeling framework was also shown to reproduce trends observed in previous idealized simulations over anisotropic porous materials, which have the potential to yield larger drag reductions than riblets: theoretical predictions and simulations suggests that anisotropic porous materials can generate up to 25% drag reduction, while riblets have been shown to produce drag reductions of up to 10%. A complementary experimental effort aimed to design, fabricate, and test the effect of porous materials with properties (i.e., porosity and permeability values) identified in previous simulations --- and in model predictions --- as giving rise to drag reduction. Due to 3D-printing constraints, it was not possible to manufacture materials with properties in the drag-reducing regime at the scale required for laboratory experiments. Nevertheless, laboratory turbulent boundary layer experiments demonstrated that the high-porosity 3D printed materials led to minimal increases in friction, which was consistent with expectations. To our knowledge, these experiments constitute the first tests over 3D-printed porous materials designed for turbulent drag reduction.

Finally, research supported by this grant has generated several domestic and international academic collaborations as well as interactions with emerging riblet manufacturing companies.

3.2 Development of Human Resources

This award provided support for Dr. Christoph Efstathiou and Dr. Andrew Chavarin, both of whom successfully defended their PhD theses in 2020. Christoph Efstathiou was primarily responsible for the experimental component of the research. Andrew Chavarin led the model development effort. After graduation, Andrew Chavarin was supported as a postdoctoral scholar on the grant for a period of 8 months and worked to extend the solvent framework to 3D riblets. Andrew Chavarin also visited the University of Cambridge in Summer 2019 with support from the US Air Force International Student Exchange Program. An outstanding set of undergraduate students helped with the experimental component of the research effort under internal support: Anika Todt, Zach Begland, Stara Shinsato, and Jefferson Nguyen.

References

- Bechert, D. W., Bruse, M., Hage, W. V., Van der Hoeven, J. T., & Hoppe, G. (1997). Experiments on drag-reducing surfaces and their optimization with an adjustable geometry. *Journal of fluid mechanics*, 338, 59-87.
- Breugem, W. P., Boersma, B. J., & Uittenbogaard, R. E. (2006). The influence of wall permeability on turbulent channel flow. *Journal of Fluid Mechanics*, 562, 35-72.
- Chavarin, A., & Luhar, M. (2020). Resolvent analysis for turbulent channel flow with riblets. *AIAA Journal*, 58(2), 589-599.
- Chavarin, A., Efstathiou, C., Vijay, S., & Luhar, M. (2020). Resolvent-based design and experimental testing of porous materials for passive turbulence control. *International Journal of Heat and Fluid Flow*, 86, 108722.
- Chavarin, A., Gomez-de-Segura, G., Garcia-Mayoral, R., & Luhar, M. (2021). Resolvent-based predictions for turbulent flow over anisotropic permeable substrates. *Journal of Fluid Mechanics*, 913, A24.
- Efstathiou, C., & Luhar, M. (2018). Mean turbulence statistics in boundary layers over high-porosity foams. *Journal of Fluid Mechanics*, 841, 351-379.
- Efstathiou, C., & Luhar, M. (2020). Turbulent boundary layers over streamwise-preferential porous materials. *arXiv preprint arXiv:2006.00182*.
- Garcia-Mayoral, R., & Jimenez, J. (2011). Hydrodynamic stability and breakdown of the viscous regime over riblets. *Journal of Fluid Mechanics*, 678, 317-347.
- Gómez-de-Segura, G., Sharma, A., & García-Mayoral, R. (2018). Turbulent drag reduction using anisotropic permeable substrates. *Flow, Turbulence and Combustion*, 100(4), 995-1014.
- Gómez-de-Segura, G., & García-Mayoral, R. (2019). Turbulent drag reduction by anisotropic permeable substrates-analysis and direct numerical simulations. *Journal of Fluid Mechanics*, 875, 124-172.
- Luhar, M., Sharma, A. S., & McKeon, B. J. (2014). Opposition control within the resolvent analysis framework. *Journal of Fluid Mechanics*, 749, 597-626.
- Marusic, I., Mathis, R., & Hutchins, N. (2010). Predictive model for wall-bounded turbulent flow. *Science*, 329(5988), 193-196.
- McKeon, B. J., & Sharma, A. S. (2010). A critical-layer framework for turbulent pipe flow. *Journal of Fluid Mechanics*, 658, 336-382.
- McClure, P. D., Smith, B. R., & Baker, W. (2020). Design and testing of 3-D riblets. In *AIAA Scitech 2020 Forum* (p. 0311).
- Nakashima, S., Fukagata, K., & Luhar, M. (2017). Assessment of suboptimal control for turbulent skin friction reduction via resolvent analysis. *Journal of Fluid Mechanics*, 828, 496-526.

- Rosti, M. E., Brandt, L., & Pinelli, A. (2018). Turbulent channel flow over an anisotropic porous wall—drag increase and reduction. *Journal of Fluid Mechanics*, 842, 381-394.
- Smits, A. J., McKeon, B. J., & Marusic, I. (2011). High-Reynolds number wall turbulence. *Annual Review of Fluid Mechanics*, 43.